CrossMark

Hydrogen Production from Methane Decomposition in Cold Plasma Reactor with Rotating Electrodes

Mohammad Mahdi Moshrefi[1] · **Fariborz Rashidi**[1]

Abstract Methane decomposition in plasma reactor is a green process and can be considered as an economical route to produce CO_x-free hydrogen. The present study aimed to design and construct a plasma reactor with a unique feature of stable operation to provide an opportunity for direct decomposition of methane at almost ambient temperature. The reactor performance was evaluated in terms of hydrogen selectivity and methane conversion under various feed flow rate, plasma power, and electrode velocity. The main product was hydrogen with a small amount of C_2 hydrocarbons where C_2 refers to ethane, ethylene, and acetylene. In addition, the role of the degree of non-equilibrium state in plasma reactor performance was studied to provide a better understanding of the complex behavior of the cold plasma reactor. Better performance was observed through the rotation of high voltage electrode, compared to fixed electrode in terms of methane conversion attributed to the uniform dispersion of plasma power and effective distribution of active species.

Introduction

Economy and environment are regarded as two main concerns in the energy sector with respect to sustainability issues. Hydrogen is an important source of green energy and methane, the major constituent of natural gas, is a good source of hydrogen due to its high hydrogen to carbon atom ratio and its availability. The decomposition of methane can result in producing the added value product of hydrogen and solid carbon. Methane decomposition into hydrogen and solid carbon directly cannot play any significant role in

✉ Fariborz Rashidi
rashidi@aut.ac.ir

1 Chemical Engineering Department, Amirkabir University of Technology, 424 Hafez Ave, Tehran, Iran

global warming since this process is free from CO_x emission. Many experts believe that hydrogen is the main candidate for sustainable and clean energy in near future. In addition, hydrogen is considered as one of the alternatives for an energy carrier with respect to energy storage issues [1]. Hydrogen is conventionally produced through steam reforming of hydrocarbons. As high CO_2 emission is a major environmental problem facing steam reforming these days, catalytic methane decomposition seems to be a suitable alternative. Catalysts such as iron [2], ceria, zirconia and lanthana supported nickel [3], nickel-copper based [4], silica porous solids [5], carbon active [6] and the like have been investigated for this purpose comprehensively. Generally, catalytic decomposition of methane requires high heat that leads to emit large amounts of CO_2 by itself. Further, catalyst forces the process design to consider pretreatment unit for gas purification due to catalyst poisoning and deactivation problems. Research and development in plasma technology have opened a new window for hydrogen industry. Plasma reactor, as an emerging technology could be regarded as a clean alternative to produce hydrogen from methane decomposition. However, direct decomposition of methane into hydrogen and solid carbon by plasma reactor poses some challenges such as energy efficiency. A large number of studies have been conducted for reforming of hydrocarbons by using plasma reactors [7–11]. Some works used a hybrid system of plasma and catalyst [12–14] while others used only plasma [15–17].

Furthermore, regarding target products, some studies emphasized the production of C_2 hydrocarbons and hydrogen [18–20], while some considered the carbon as added value product [21–23]. Considering all the aforementioned studies, the present study aimed to develop a new type of plasma reactor with rotating electrodes which can guarantee stable operation and moderately increase the degree of the non-equilibrium state. In this reactor, the plasma zone is rotated due to the external rotary force imposed on high voltage and ground electrodes which can pave the way for evaluating the effect of operating parameters such as feed flow rate, plasma power, and velocity of arc rotation more independently. It is worth noting that the present design has some conceptual differences with those reported by other researchers [24, 25]. Regarding the previous studies, the arc was rotated by the force of fluid flow and accordingly there was a high order of dependency and interaction among operating parameters. In addition, only the ground electrode was rotating and arc discharge was fixed in the previous version of the current reactor [26–29]. However, in the present study, a more homogeneous discharge is obtained due to arc rotation leading to more stable operation as well as increasing energy efficiency.

Experimental Set Up

Experimental setup includes feed supply system, power supply system and reactor. Gas cylinders (Farafan Gas, Iran), mass flow controller (Brooks 5850), steel tubes, on/off valves and connections are regarded as the parts of feed supply system. Transformer voltage (AC, up to 12 kV, manufactured by Yeganeh-trance, Iran) was controlled by variable auto-trans and the output voltage of the transformer was manually coupled by diode and capacitor in the laboratory for providing direct current (DC). Due to high electrical conductivity of plasma zone, reactor and ballast resistance (1 MΩ) were connected in series in order to prevent sudden current increase which could damage the transformer. Figure 1 illustrates a schematic plan of electrical diagram and experimental set-up. Methane and Argon were both 99.999% pure and were supplied from separate gas
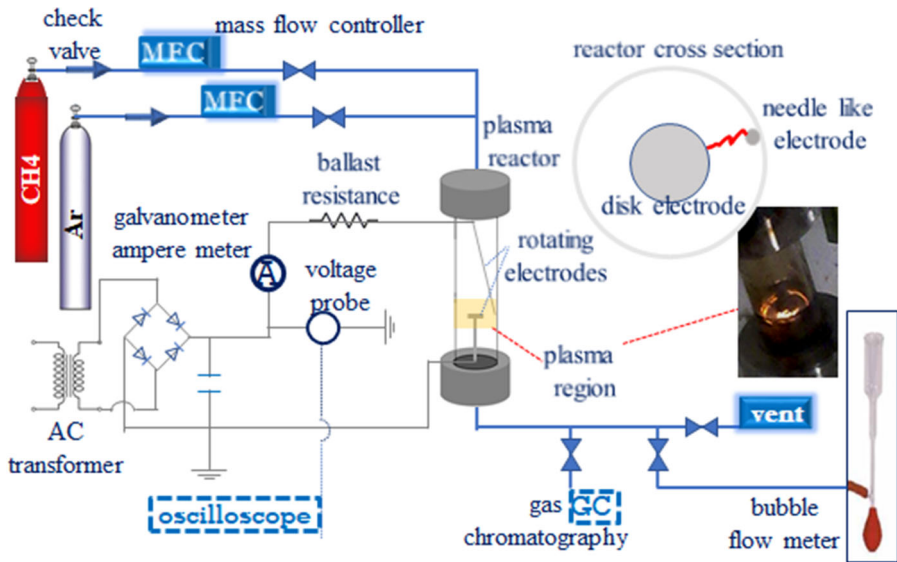
Fig. 1 Schematic of experimental set up and reactor structure

tanks by mass flow controllers and perfectly mixed before flowing into the plasma zone of the reactor where ionized gas exists. In all of the experiments, the feed entered the reactor at the room temperature of 28–30 °C and atmospheric pressure. In addition, argon was used in material balance calculations and diluting the gaseous stream for gas chromatography. Further, input and output flow rates of reactor were measured by bubble flow meter. Furthermore, plasma power measuring system included high voltage probe (PINTEK HVP-39pro), oscilloscope (GW Instek, GOS-620), and galvanometer ammeter. The produced gas was directed to the inline-calibrated gas chromatograph (GC, Agilent, 6890 N) for composition analysis. Generally, plasma reactors are known to have rapid startup time. However, each sample was injected to the GC about 7 min after reactor startup to confirm the lines were thoroughly washed up by produced gas. The GC had a flame ionization detector (FID) as well as a thermal conductivity detector (TCD). In addition, the present study focused on the effect of the degree of non-equilibrium state on methane conversion and product selectivity. To this aim, the current plasma reactor was designed and constructed with rotating electrodes. Reactor structure is displayed in Fig. 1. The reactor is a quartz tube with 30 mm OD, 26 mm ID and 150 mm length, which is equipped with two stainless steel (SS) electrodes including needle like (high voltage electrode) and disk type (ground electrode). The electrodes are 6 mm apart and are placed opposite to each other. The diameter of ground electrode is 10 mm and both electrodes are connected to a DC motor shaft by joint bush passing through a flange. In order to seal properly, the rotating shaft goes through a mechanical seal and an O-ring is placed between the quartz tube and stainless-steel flange. DC motor drivers provide 0–6000 rpm velocity for electrodes. Further, methane conversion, hydrogen selectivity, energy efficiency and C_2 hydrocarbons selectivity were selected for evaluation. Hydrogen selectivity and C_2 hydrocarbons selectivity are defined in terms of hydrogen base and carbon base. Further, the present study investigated the effect of plasma power and feed flow rate variations which can play a significant role in plasma chemistry. In addition, the structure of the present reactor

provides opportunity to study the degree of non-equilibrium state by changing high voltage electrode velocity. Factorial method was selected to design experiments due to high interaction between input parameters and unknown nature of the process happening in the plasma zone. Three different powers and flow rates were selected while high voltage electrode velocity could be tuned from 0 up to 6000 RPM. It is worth noting that the consumed power by plasma is not really a fully independent input parameter as it relies on the resistance of the formed plasma apart from the decision made by the operator. For example, it was impossible to achieve 7 W at high feed flow rates and unstable discharge occurred at high electrode velocities in low powers. In other words, a full range (0–6000 rpm) of electrode velocity was not practically implemented.

Results and Discussion

In the process of methane decomposition, the collisions between energetic electrons and CH_4 molecules result in creating either active species which continue further reactions or forming products. Hydrogen is a major constituent of gaseous product with little amount of C_2 hydrocarbons while carbon is deposited in a solid phase. Plasma chemistry has a complex nature due to electron collisions as well as standard thermodynamic reactions. Electron impacts create active species while reactions among radicals are related to standard thermodynamic reactions. In order to interpret the experimental results, the reaction zone is supposed to involve plasma zone where the reactions of electron collision are dominant, along with the recombination of active species with each other or initiation of new elementary reactions. In addition, carbon atoms in the plasma zone will be deposited as solid carbon and hydrogen radicals existing in the plasma zone, result in initiating thermodynamic reactions.

Reaction Pathway

Excitation, ionization and dissociation are regarded as the main reactions in plasma zone. Electron collisions provide ions and a cascade of electrons, which create an electrical conductive gas zone called "plasma". Excitation rate of methane and ethane decomposition is insignificant in atmospheric pressure plasma jet [17]. In addition, in order to reduce the complexity, only dissociation reactions are considered, irrespective of ionization reactions in the present study.

In order to construct a simple representative reaction pathway, the equilibrium concentration of probable species were considered as well as standard thermodynamic reaction pathway analysis based on kinetic suggested by Sinaki et al. [30]. As illustrated in Figs. 2 and 3, the equilibrium concentrations of H_2, H, CH, CH_2, C_2H, CH_3, C_2H_2, C_2H_4, C_2H_6, CH_4, C(S) and C(g) species versus temperature were numerically calculated for dissociating 1 mol of methane by using Gibbs energy minimization. It is worth noting that only the concentration of major species is displayed in these figures. In addition, they imply that no tendency is available to form C_2 hydrocarbons if the required conditions for carbon nucleation are provided (Fig. 2). Alternatively, the chemical equilibrium tends toward the formation of C_2 hydrocarbons if the required conditions for carbon nucleation are not provided (Fig. 3). Theoretically, solid carbon can be formed by electron impacts or standard thermodynamic reaction in plasma zone. In addition, the accepted mechanisms for carbon formation by radical reactions are based on the polycyclic aromatic hydrocarbons
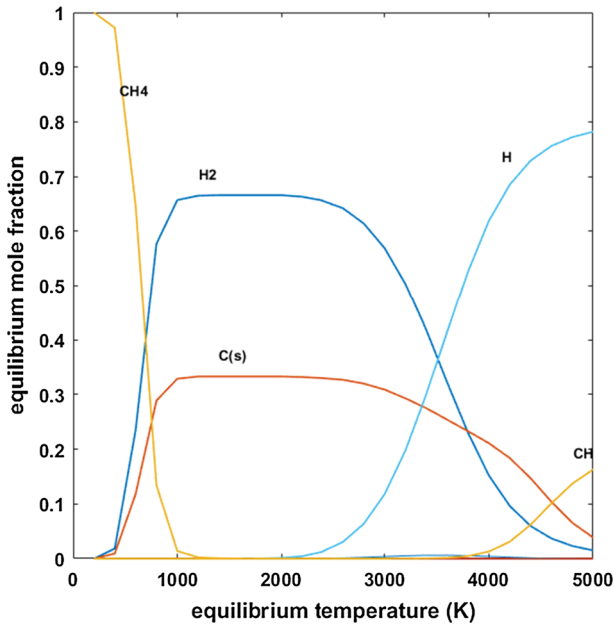
Fig. 2 Equilibrium concentration of major probable species if carbon nucleation is allowed
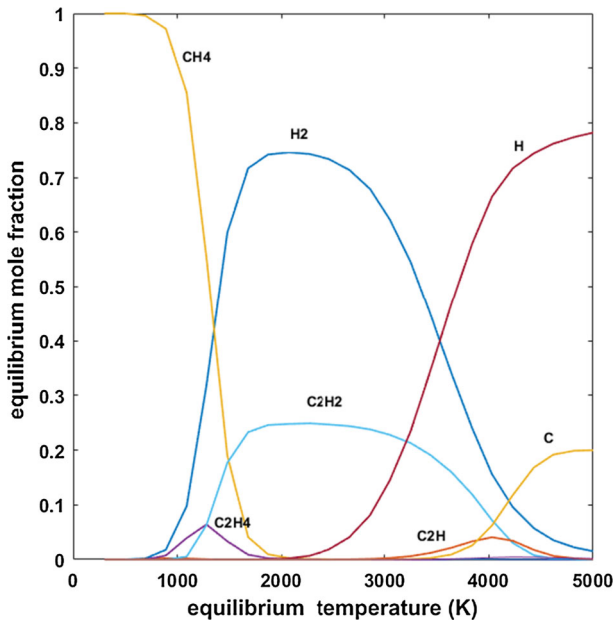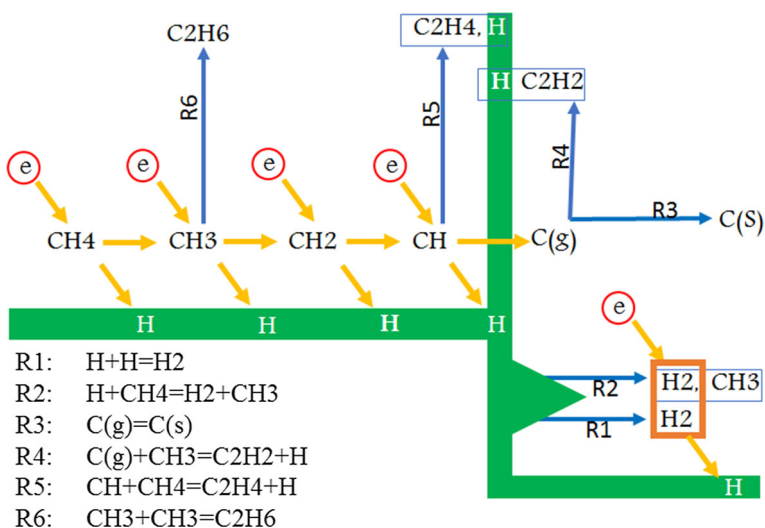

Fig. 3 Equilibrium concentration of major probable species if carbon nucleation is not allowed

(PAHs) or C_2H_2 formation [31, 32]. However, both temperature and residence time are rather low in plasma zone of the reactor and PAH and C_2H_2 would be stable with no chance to undergo carbon nucleation to form solid carbon for deposition in the case of producing. Therefore, electron impacts are responsible for carbon deposition, i.e., breakage of methane molecular bonds by electron collisions. Based on the aforementioned analysis, the reaction pathway is proposed for methane decomposition in the plasma zone of the reactor (Fig. 4). Based on this pathway, dissociation reactions (orange arrows in Fig. 4) are responsible for solid carbon deposition while, the production of C_2 hydrocarbons is related to standard thermodynamic reactions (blue arrows in Fig. 4). The produced hydrogen (as target product) may again dissociate into atomic hydrogen by electron collision. It is worth noting that the required energy to break methane bonds is not supplied by a high temperature heat source in a cold plasma reactor while the collisions between energetic electrons and methane molecules create active species in the plasma region that these species have ability to initiate thermodynamic reactions at even near ambient temperatures. In conclusion, the role of plasma as the catalyst is confirmed based on the results.
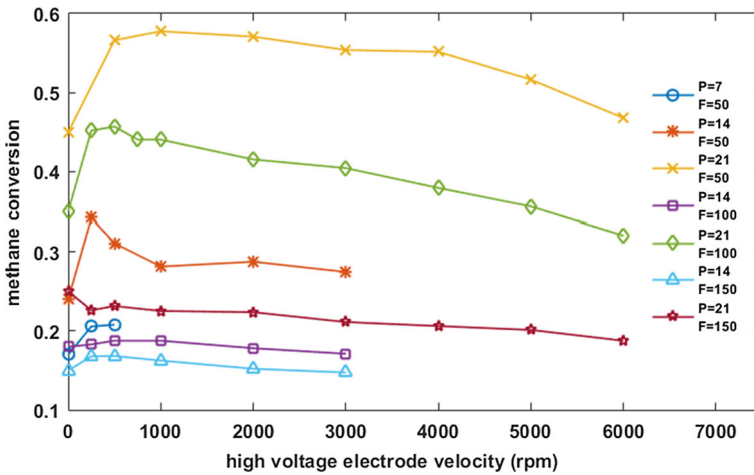
Methane Conversion

Figure 5 illustrates methane conversion at different stable operation conditions of feed flow rate, plasma power and electrode velocity. Increasing power and reducing flow rate result in increasing in methane conversion. In addition, the effect of power on conversion rise is emphasized as flow rate decreases,

By using the reactor of this study including rotating electrodes, the effect of the degree of non-equilibrium state can be investigated. Regarding the comparison of the results of plasma reactor with rotating arc discharge in the present study with those of stationary arc discharge in the previous study [29], methane conversion increases significantly, due to approaching non-equilibrium state at plasma zone. Generally, the time scale for plasma reactions is extremely short (nano seconds) [33]. Hence, hydrogen as the target product is created when electrical discharge occurs (e.g., $CH_4 + e = CH_3 + H + e$ followed by

R1:   H+H=H2
R2:   H+CH4=H2+CH3
R3:   C(g)=C(s)
R4:   C(g)+CH3=C2H2+H
R5:   CH+CH4=C2H4+H
R6:   CH3+CH3=C2H6

Fig. 4 Simple representative reaction path way of methane decomposition in this study

Fig. 5 Conversion of methane versus electrode velocity at various methane flow rate; F (cm^3/min) and power; P (watts). Methane is always diluted by 50 cm^3/min argon

H + H = H$_2$). Consequently, an increase takes place in local H$_2$ concentration at discharge zone leading to an increase in the probability of undesirable reaction of hydrogen dissociation (i.e., H$_2$ + e = H + H + e) instead of desirable electron collisions with reactant (CH$_4$) molecules. In addition, the zone away from electrical discharge cannot participate in the reactions effectively. However, the rotation of the high voltage electrode leads to the occurrence of arc rotation and a better distribution of species and consequently higher conversions. Figure 6 illustrates a schematic plan of the aforementioned idea. The fixed and rotating discharge responses are demonstrated in terms of local concentration of


(a) Stationary arc discharge   **(b)** Rotating arc discharge

— **Hydrogen molecule**
✗ **Methane molecule**
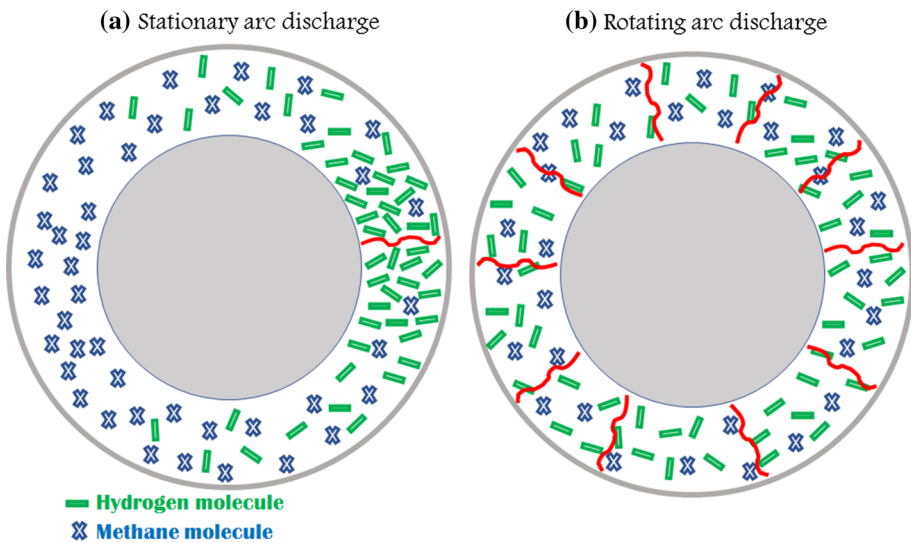
Fig. 6 Hypothetical schematics representing H$_2$ and CH$_4$ molecules distribution for **a** stationary arc discharge and **b** rotating arc discharge

methane as a reactant and hydrogen as a product. As shown in Fig. 6, local methane concentration is low for fixed electrode case and local hydrogen concentration is high in discharge zone which suggest the vicinity of equilibrium state. On the other hand, high voltage electrode rotation will cause only ions to accompany plasma zone due to the force of electrical field and neutral species such as hydrogen molecules leave discharge zone, along with the undesirable reactions of electron collision with them is relatively prevented. In fact, lower methane conversion occurs due to nonhomogeneous distribution of species when high voltage electrode is fixed while the rotation of high voltage electrode causes the simultaneous rotation of charged particles which alternately places charged particles in an environment with high concentration of raw feed. In other words, an increase happens in the non-equilibrium degree. Therefore, the rotation of the charged particles is responsible for active radicals to stay behind discharge zone where they can react with other species and set up the fresh plasma zone in order to produce active species. Consequently, a more homogenous discharge is achieved. In addition, it is worth noting that high voltage electrode rotation has other advantages such as making the arc channel longer, preventing full arc to establish and keeping arc channel in less thermal state which are considered as some reasons for higher conversions.

Product Distribution

Hydrogen as an atom or a molecule is responsible for a majority of radical reactions. In fact, produced hydrogen radicals undergo many reaction paths. Figure 4 illustrates the radicals to form hydrogen molecule and reacting with methane to form hydrogen molecule and methyl radical. In addition, hydrogen selectivity and yield are illustrated in Figs. 7 and
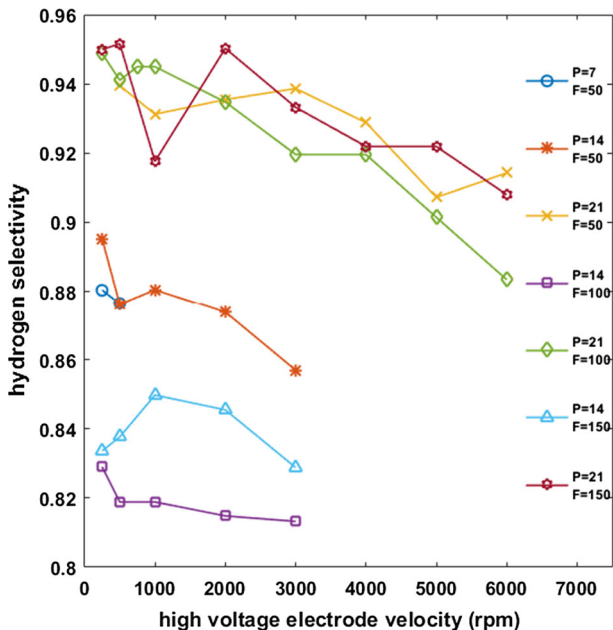
Fig. 7 Hydrogen selectivity versus electrode velocity at various methane flow rate; F (cm^3/min) and power; P (watts). Methane is always diluted by 50 cm^3/min argon
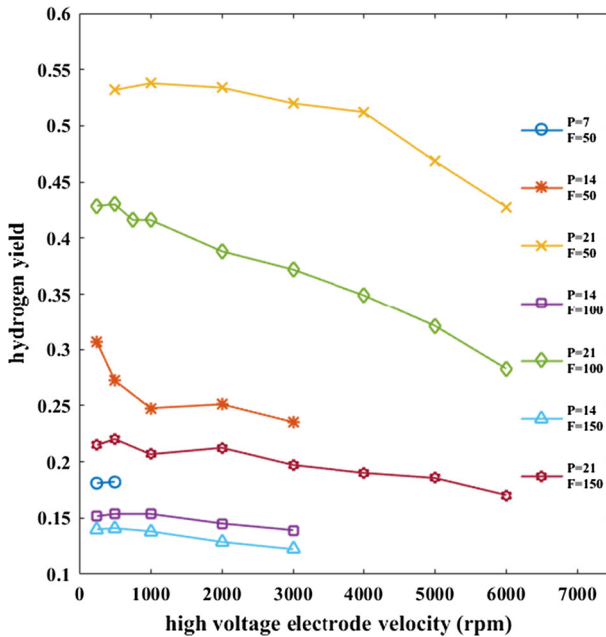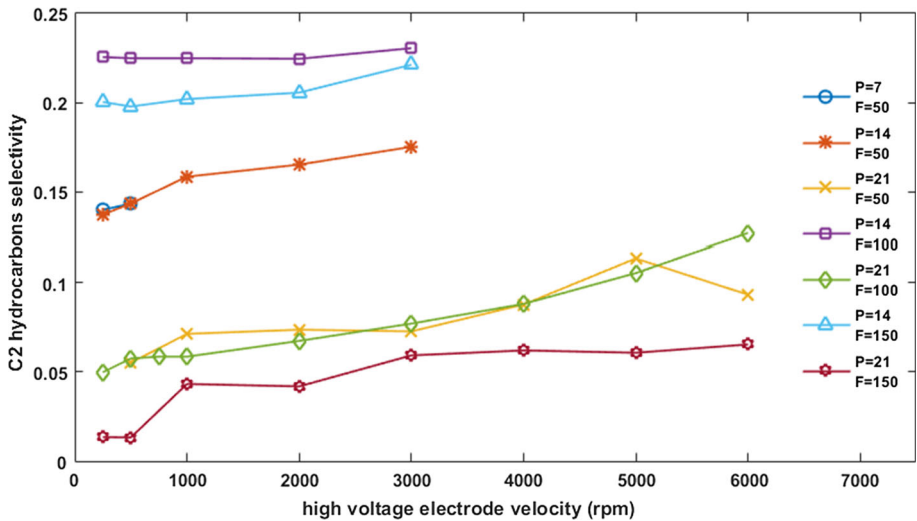
Fig. 8 Hydrogen yield versus electrode velocity at various methane flow rate; F (cm^3/min) and power; P (watts). Methane is always diluted by 50 cm^3/min argon

8, respectively. An increase in power at a fixed feed flow rate condition leads to an increase in hydrogen selectivity. The proposed reaction pathway confirms this behavior. At low powers, CH$_x$ radicals have high concentration in the reaction zone and the quantity and energy of electrons increase by increasing power which in turn causes more production of hydrogen. Figure 8 displays the hydrogen yield and the domination of the conversion. In addition, feed flow rate and plasma power play an inverse effect on yield. Thus, the effects should be considered simultaneously for better yields. Further, the dissociation reactions lead to the formation of CH$_x$ radicals. We propose CH$_3$ and CH$_2$ radicals should be rapidly consumed by electron impacts and accordingly their local concentrations are considerably lower than those of CH radicals. Although a majority of CH radicals decomposes into carbon and hydrogen, some will form C$_2$H$_4$ through reaction with methane, confirmed by the experimental results as C$_2$H$_4$ was the main produced hydrocarbon. According to the aforementioned and proposed reactions pathway, the concentration order of C$_2$ hydrocarbons should be as C$_2$H$_4$ > C$_2$H$_6$ > C$_2$H$_2$ which is consistent with the obtained experimental results.

Based on the reaction pathway, CH$_3$, CH$_2$ and CH radicals are responsible for C$_2$ hydrocarbons selectivity (Fig. 9). These radicals are consumed by electron collisions as well as thermodynamic reactions (R4–R6 in Fig. 4) to produce hydrogen radicals and C$_2$ hydrocarbons. It is worth noting that the rate of electron collision reaction depends on electron density and electron energy, which could be represented by power. Thus, increasing power can promote electron collision reactions (conversion of CH$_x$ radicals into CH$_{x-1}$) leading to a decrease in C$_2$ hydrocarbons selectivity. On the other hand, any factor which can withdraw CH$_x$ radicals from the discharge zone will promote R4–R6 reactions which is regarded as the main reason for higher production of C$_2$ hydrocarbons due to an

Fig. 9 C_2 hydrocarbons selectivity versus electrode velocity at various methane flow rate; F (cm^3/min) and power; P (watts). Methane is always diluted by 50 cm^3/min argon

increase in feed flow rate. The same argument can be valid for higher production of C2 hydrocarbons at the elevated electrode velocities which results in decreasing hydrogen selectivity. It is worth noting that any decrease in C_2 hydrocarbons selectivity on carbon base suggests a progression of reactions toward more solid carbon formation (Fig. 10). The
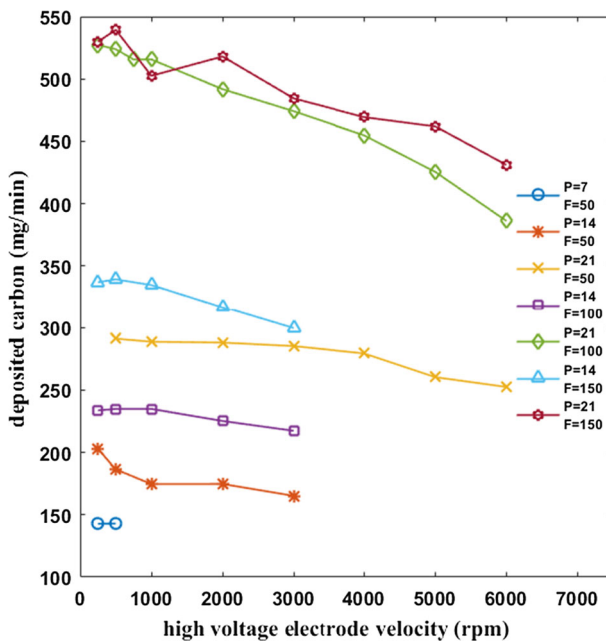
Fig. 10 Deposited carbon versus electrode velocity at various methane flow rate; F (cm^3/min) and power; P (watts). Methane is always diluted by 50 cm^3/min argon

produced carbon in gaseous phase reacts with either CH_2 or CH_3 radicals to form C_2H_2 while most is deposited in solid phase.

Energy Efficiency

Energy efficiency is defined as the number of moles of converted methane divided by the required input power for conversion as represented in Eq. 1 [34]:

$$\eta = \frac{CH_4 \; converted}{P} \tag{1}$$

All electron collisions are not really fully effective due to (a) various energy losses, especially joule heating, i.e., performance of electrons discharge as a heat source, and (b) colliding the electrons with hydrogen molecules undesirably. Approaching non-equilibrium state from quasi-equilibrium state of plasma results in more efficient performance. Therefore, attempts should be made to evaluate various practical designs in order to obtain a high order of non-equilibrium state.

Rotating electrodes is based on the presented idea in the present study. Table 1 represents energy efficiency for rotating high voltage plasma reactor as the function of power and flow rate indicating 20% increase (maximum efficiency is around 1.46 mol/kJ), compared to stationary high voltage electrode (maximum energy efficiency of around 1.21 mol/kJ [29]) due to higher methane conversion at constant hydrogen selectivity for rotating electrode reactor.

Conclusion

The present study aimed to present methane decomposition to hydrogen and solid carbon in a continuous plasma reactor with rotating electrodes. The presented new structure causes stable operation. A reaction pathway was proposed which attributes formation of atomic hydrogen and carbon to electron dissociation reactions while the formation of hydrogen molecules was attributed to standard thermodynamic reactions. Based on the results, the plasma could possess catalyst property, as it caused some reactions to happen at considerably lower temperatures due to the generation of sufficient reactive species for reaction

Table 1 Methane conversion and energy efficiency for rotating arc discharge plasma reactor

Methane flow rat (cm^3/min)	Plasma power (W)	Methane conversion (%)		Energy efficiency (mmole/kJ)	
		Fixed HV electrode	Rotating HV electrode	Fixed HV electrode	Rotating HV electrode
50	7	17	20	0.82	0.97
50	14	24	35	0.58	0.85
50	21	45	59	0.73	0.95
100	14	18	20	0.87	0.97
100	21	35	45	1.13	1.46
150	14	15	18	1.09	1.31
150	21	25	24	1.21	1.16

initiation and provided additional adjustable parameters toward selective production. Further, plasma state approached non-equilibrium by rotating high voltage electrode. Accordingly, the catalytic role was more pronounced which is beneficial in terms of energy efficiency as a major challenge facing methane decomposition. Finally, methane conversion and energy efficiency are improved compared to fixed high voltage electrode and reached around 60% and 1.46 mol/kJ respectively.

References

1. Amirante R, Cassone E, Distaso E, Tamburrano P (2017) Overview on recent developments in energy storage: mechanical, electrochemical and hydrogen technologies. Energy Convers Manag 132:372–387
2. Zhou L, Enakonda LR, Harb M, Saih Y, Aguilar-Tapia A, Ould-Chikh S, J-l Hazemann, Li J, Wei N, Gary D (2017) Fe catalysts for methane decomposition to produce hydrogen and carbon nano materials. Appl Catal B 208:44–59
3. Pudukudy M, Yaakob Z, Takriff MS (2016) Methane decomposition into COx free hydrogen and multiwalled carbon nanotubes over ceria, zirconia and lanthana supported nickel catalysts prepared via a facile solid state citrate fusion method. Energy Convers Manag 126:302–315
4. Shen Y, Lua AC (2015) Polyol synthesis of nickel–copper based catalysts for hydrogen production by methane decomposition. Int J Hydrogen Energy 40(1):311–321
5. Serrano DP, Botas JA, Pizarro P, Moreno I, Gomez G (2015) Hydrogen production through catalytic methane decomposition promoted by pure silica materials. Int J Hydrogen Energy 40(15):5237–5243
6. Al-Hassani AA, Abbas HF, Daud WW (2014) Production of CO_x-free hydrogen by the thermal decomposition of methane over activated carbon: catalyst deactivation. Int J Hydrogen Energy 39(27):14783–14791
7. Shapoval V, Marotta E (2015) Investigation on plasma-driven methane dry reforming in a self-triggered spark reactor. Plasma Processes Polym 12(8):808–816
8. Horvath G, Zahoran M, Mason N, Matejcik S (2011) Methane decomposition leading to deposit formation in a DC positive CH_4–N_2 corona discharge. Plasma Chem Plasma Process 31(2):327–335
9. Hsieh L-T, Lee W-J, Chen C-Y, Chang M-B, Chang H-C (1998) Converting methane by using an RF plasma reactor. Plasma Chem Plasma Process 18(2):215–239
10. Lee DH, Song Y-H, Kim K-T, Lee J-O (2013) Comparative study of methane activation process by different plasma sources. Plasma Chem Plasma Process 33(4):647–661
11. Li T, Rehmet C, Cheng Y, Jin Y, Cheng Y (2017) Experimental comparison of methane pyrolysis in thermal plasma. Plasma Chem Plasma Process 37(4):1033–1049
12. Ghorbani Z, Parvin P, Reyhani A, Mortazavi S, Moosakhani A, Maleki M, Kiani S (2014) Methane decomposition using metal-assisted nanosecond laser-induced plasma at atmospheric pressure. J Phys Chem C 118(51):29822–29835
13. Rahimpour M, Jahanmiri A, Shirazi MM, Hooshmand N, Taghvaei H (2013) Combination of non-thermal plasma and heterogeneous catalysis for methane and hexadecane co-cracking: effect of voltage and catalyst configuration. Chem Eng J 219:245–253
14. Ogata A, Mizuno K, Kushiyama S, Yamamoto T (1998) Methane decomposition in a barium titanate packed-bed nonthermal plasma reactor. Plasma Chem Plasma Process 18(3):363–373
15. Da Silva C, Ishikawa T, Santos S, Alves C, Martinelli A (2006) Production of hydrogen from methane using pulsed plasma and simultaneous storage in titanium sheet. Int J Hydrogen Energy 31(1):49–54
16. Lotfalipour R, Ghorbanzadeh A, Mahdian A (2014) Methane conversion by repetitive nanosecond pulsed plasma. J Phys D Appl Phys 47(36):365201
17. Sanchez-Gonzalez R, Kim Y, Rosocha LA, Abbate S (2007) Methane and ethane decomposition in an atmospheric-pressure plasma jet. IEEE Trans Plasma Sci 35(6):1669–1676
18. Yang Y (2003) Direct non-oxidative methane conversion by non-thermal plasma: modeling study. Plasma Chem Plasma Process 23(2):327–346
19. Morgan NN, ElSabbagh M (2017) Hydrogen production from methane through pulsed DC plasma. Plasma Chem Plasma Process 37(5):1375–1392
20. Yang Y (2003) Direct non-oxidative methane conversion by non-thermal plasma: experimental study. Plasma Chem Plasma Process 23(2):283–296

21. Pristavita R, Mendoza-Gonzalez N-Y, Meunier J-L, Berk D (2010) Carbon blacks produced by thermal plasma: the influence of the reactor geometry on the product morphology. Plasma Chem Plasma Process 30(2):267–279
22. Pristavita R, Meunier J-L, Berk D (2011) Carbon nano-flakes produced by an inductively coupled thermal plasma system for catalyst applications. Plasma Chem Plasma Process 31(2):393–403
23. Okeke L, Störi H (1991) Plasma-chemical decomposition of methane during diamond synthesis. Plasma Chem Plasma Process 11(4):489–499
24. Li XD, Zhang H, Yan SX, Yan JH, Du CM (2013) Hydrogen production from partial oxidation of methane using an AC rotating gliding arc reactor. IEEE Trans Plasma Sci 41(1):126–132
25. Zhang H, Du C, Wu A, Bo Z, Yan J, Li X (2014) Rotating gliding arc assisted methane decomposition in nitrogen for hydrogen production. Int J Hydrogen Energy 39(24):12620–12635
26. Moshrefi MM, Rashidi F (2014) Hydrogen production from methane by DC spark discharge: effect of current and voltage. J Nat Gas Sci Eng 16:85–89
27. Moshrefi MM, Rashidi F, Bozorgzadeh HR (2015) Use of a DC discharge in a plasma reactor with a rotating ground electrode for production of synthesis gas by partial oxidation of methane. Res Chem Intermed 41(9):5941–5959
28. Moshrefi MM, Rashidi F, Bozorgzadeh HR, Haghighi ME (2013) Dry reforming of methane by DC spark discharge with a rotating electrode. Plasma Chem Plasma Process 33(2):453–466
29. Moshrefi MM, Rashidi F, Bozorgzadeh HR, Zekordi SM (2012) Methane conversion to hydrogen and carbon black by DC-spark discharge. Plasma Chem Plasma Process 32(6):1157–1168
30. Younessi-Sinaki M, Matida EA, Hamdullahpur F (2009) Kinetic model of homogeneous thermal decomposition of methane and ethane. Int J Hydrogen Energy 34(9):3710–3716
31. Dors M, Nowakowska H, Jasiński M, Mizeraczyk J (2014) Chemical kinetics of methane pyrolysis in microwave plasma at atmospheric pressure. Plasma Chem Plasma Process 34(2):313–326
32. Fincke JR, Anderson RP, Hyde T, Detering BA, Wright R, Bewley RL, Haggard DC, Swank WD (2002) Plasma thermal conversion of methane to acetylene. Plasma Chem Plasma Process 22(1):105–136
33. Kim H-H, Teramoto Y, Ogata A, Takagi H, Nanba T (2016) Plasma catalysis for environmental treatment and energy applications. Plasma Chem Plasma Process 36(1):45–72
34. Long H, Shang S, Tao X, Yin Y, Dai X (2008) CO_2 reforming of CH_4 by combination of cold plasma jet and Ni/γ-Al_2O_3 catalyst. Int J Hydrogen Energy 33(20):5510–5515